Modeling and performance metrics of MIMO-SDM systems with different amplification schemes in the presence of mode-dependent loss

Cristian Antonelli,[1,*] **Antonio Mecozzi,**[1] **Mark Shtaif,**[2] **and Peter J. Winzer**[3]

[1] *Dept. of Physical and Chemical Sciences, University of L'Aquila, 67100 L'Aquila, Italy*
[2] *School of Electrical Engineering, Tel Aviv University, Tel Aviv, Israel 69978*
[3] *Bell Labs, Alcatel-Lucent, 791 Holmdel-Keyport Rd., Holmdel, New Jersey 07733, USA*
[*] *cristian.antonelli@univaq.it*

Abstract: Mode-dependent loss (MDL) is a major factor limiting the achievable information rate in multiple-input multiple-output space-division multiplexed systems. In this paper we show that its impact on system performance, which we quantify in terms of the capacity reduction relative to a reference MDL-free system, may depend strongly on the operation of the inline optical amplifiers. This dependency is particularly strong in low mode-count systems. In addition, we discuss ways in which the signal-to-noise ratio of the MDL-free reference system can be defined and quantify the differences in the predicted capacity loss. Finally, we stress the importance of correctly accounting for the effect of MDL on the accumulation of amplification noise.

© 2015 Optical Society of America

OCIS codes: (060.2330) Fiber optics communications; (060.4510) Optical communications; (060.4230) Multiplexing.

References and links

1. P. J. Winzer and G. J. Foschini, "MIMO capacities and outage probabilities in spatially multiplexed optical transport systems," Opt. Express **19**, 16680–16696 (2011).
2. K-P. Ho and J. M. Kahn, "Mode-dependent loss and gain: statistics and effect on mode-division multiplexing," Opt. Express **19**, 16612–16635 (2011).
3. S. Warm and K. Petermann, "Splice loss requirements in multi-mode fiber mode-division-multiplex transmission links," Opt. Express **21**, 519–532 (2013).
4. K-P. Ho and J. M. Kahn, "Frequency Diversity in Mode-Division Multiplexing Systems," IEEE J. Lightwave Technol. **29**, 3719–3726 (2011).
5. A. Andrusier, M. Shtaif, C. Antonelli, and A. Mecozzi, "Assessing the effects of mode-dependent loss in space-division multiplexed systems," IEEE J. Lightwave Technol. **32**, 1317–1322 (2014).
6. A. Juarez, E. Krune, S. Warm, C. A. Bunge, and K. Petermann, "Modeling of mode coupling in multimode fibers with respect to bandwidth and loss," IEEE J. Lightwave Technol. **32**, 1549–1558 (2014).
7. A. Andrusier, M. Shtaif, C. Antonelli, and A. Mecozzi, "Characterization of mode-dependent loss in SDM systems" Proc. OFC, Paper Th1J.2 (2014).
8. A. Lobato, F. Ferreira, M. Kuschnerov, D. van den Borne, S. L. Jansen, A. Napoli, B. Spinnler, and B. Lankl, "Impact of mode coupling on the mode-dependent loss tolerance in few-mode fiber transmission," Opt. Express **20**, 29776–29783 (2012).
9. K. Guan, P. J. Winzer, and M. Shtaif, "On the BER performance of MIMO-SDM systems with finite constellation inputs," IEEE Photon. Technol. Letters **23**, 1223–1226 (2014).

#225568 - $15.00 USD Received 24 Oct 2014; revised 2 Dec 2014; accepted 5 Dec 2014; published 28 Jan 2015
© 2015 OSA

10. A. Mecozzi and M. Shtaif, "Signal-to-noise-ratio degradation caused by polarization-dependent loss and the effect of dynamic gain equalization," IEEE J. Lightwave Technol. **22**, 1856– 1871 (2004).
11. M. Shtaif, "Performance degradation in coherent polarization multiplexed systems as a result of polarization dependent loss," Opt. Express **16**, 13918–13932 (2008).
12. J. M. Wiesenfeld, L. D. Garrett, M. Shtaif, M. H. Eiselt, R. W. Tkach, "Effects of DGE channel bandwidth on nonlinear ULH systems," OFC 2005, Paper OWA2.
13. R. N. Mahalati, D. Askarov, J. M. Kahn, "Adaptive modal gain equalization techniques in multi-mode erbium-doped fiber amplifiers," J. of Lightwave Technol. **32**, 2133 –2143 (2014).
14. A. Lobato, F. Ferreira, B. Inan, and S. Adhikari, "Maximum-likelihood detection in few-mode fiber transmission with mode-dependent loss," IEEE Photon. Technol. Lett. **25**, 1095-1098 (2013).
15. C. Antonelli, A. Mecozzi, M. Shtaif, and P. J. Winzer, "Stokes-space analysis of modal dispersion in fibers with multiple mode transmission," Opt. Express **20**, 11718–11783 (2012).
16. K-P. Ho and J.M Kahn, "Statistics of group delays in multi-mode fibers with strong mode coupling," IEEE J. Lightwave Technol. **29**, 3119–3128 (2011).
17. Q. Hu and W. Shieh, "Autocorrelation function of channel matrix in few-mode fibers with strong mode coupling," Opt. Express **21**, 22153–22165 (2013).
18. The limit of large SNR implies that the capacity $C = \log_2\left[\det\left(\mathbf{I}+S_0\mathbf{T}\mathbf{T}^\dagger\mathbf{Q}^{-1}\right)\right]$, where $\mathbf{T}$ is the channel transfer matrix and $\mathbf{Q}$ is the noise coherency matrix, can be approximated as $\log_2\left[\det\left(S_0\mathbf{T}\mathbf{T}^\dagger\mathbf{Q}^{-1}\right)\right]$ [5]. In this limit the MDL-induced capacity loss is independent of the SNR parameter S_0.
19. J.P. Gordon and H. Kogelnik, "PMD fundamentals: polarization mode dispersion in optical fibers," Proc. Natl. Acad. Sci. USA **97**, 4541–4550 (2000).
20. L. E. Nelson, C. Antonelli, A. Mecozzi, M. Birk, P. Magill, A. Schex, and L. Rapp, "Statistics of polarization dependent loss in an installed long-haul WDM system," Opt. Express **19**, 6790–6796 (2011)
21. P. J. Winzer and G. J. Foschini, "Optical MIMO-SDM system capacities," OFC 2014, Paper Th1J.1.
22. C.W. Gardiner, *Handbook of Stochastic Methods: for Physics, Chemistry and Natural Sciences* (Springer-Verlag, 1983).

1. Introduction

One of the most relevant concerns in the context of space-division multiplexed (SDM) transmission in optical fibers is related to the possible consequences of mode-dependent loss (MDL). This topic has been considered in a number of studies [1–9] and it extends earlier work which was done on MDL in single mode fibers (where the phenomenon is generally referred to as polarization dependent loss – PDL) [10, 11]. Similarly to the case of PDL, the main expected sources of MDL are inline optical amplifiers, mode multiplexers and demultiplexers, imperfect splices between fiber sections [3], and microscopic fiber bends [6]. Yet, in addition to early PDL studies, where the preferred metric for quantifying the system impact of PDL was the deterioration of the worst channel's signal-to noise-ratio, or of the average bit-error-ratio (BER) [11], in modern *coherent* systems it has also become customary to quantify the impact of MDL in terms of its effect on the system information capacity [1–5]. This metric turns out to be very sensitive to the assumptions that are made on how the system is modeled and operated.

In this paper we argue that the capacity reduction caused by MDL varies significantly with system aspects that have received little attention in previous MDL studies. We show that without explicitly relating to the operation mode of the inline optical amplifiers, the effect of MDL on system capacity cannot be determined with acceptable reliability, most critically in the case of low mode-count systems. Therefore, in a meaningful analysis of the capacity impact of MDL, it is important to specify how the mode averaged signal power is manipulated at the amplification sites. Up to now, different authors have made different assumptions regarding amplification [1–5]. The most common amplification scheme is that in which an inline amplifier resets the *total* signal power (over the entire WDM band) to its value at the link input. Ideally, in this regime all frequency components of the propagating signal undergo the same amplification. Another possible scenario is one where the inline amplifier resets the mode-averaged signal power to a nominal value on a per-frequency basis. This requires the amplifier to be equipped with an adaptive frequency equalization mechanism [10], similar to a dynamic gain equalizing filter (DGEF) in conventional single-mode systems [12]. In spite of the seemingly minor dif-

#225568 - $15.00 USD Received 24 Oct 2014; revised 2 Dec 2014; accepted 5 Dec 2014; published 28 Jan 2015
© 2015 OSA

ference between the two approaches, it turns out that they produce different distributions for the MDL-induced capacity loss, which is particularly important in the case of low mode-count transmission. We note that we only consider the effects of frequency equalization, whereas modal equalization, where the gain of each mode can be controlled individually [13] is not addressed in this paper.

Subsequently, we discuss the importance of clearly specifying the MDL-free system relative to which the capacity loss is evaluated. One possibility is to set the SNR of the MDL-free reference system to the ratio between the time averages of the total signal and noise powers (in all modes) measured in the MDL-impaired system. In some cases, when the MDL dynamics is too slow or when the accessible frequency range is not sufficient to allow effective averaging, the reference system SNR ends up depending on the specific MDL realization. While both definitions can be legitimate, they yield different results in terms of the MDL-induced capacity reduction, as we discuss in this paper.

Finally, we quantify the error that is incurred when the effects of MDL on the accumulated amplification noise are ignored by assuming that spatially isotropic noise is added to the transmitted signal at the receiver [2, 3].

The paper is organized as follows. In Sec. 2 we illustrate the importance of the amplification strategy when considering the MDL-induced capacity reduction. In Sec. 3 we discuss the use of the capacity loss per mode relative to a more commonly used capacity ratio when considering the impact of MDL. In Sec. 4 we discuss the importance of precisely defining the MDL-free reference system, relative to which the penalties due to MDL are evaluated, and introduce possible definitions for such reference systems. Section 5 is devoted to demonstrating the importance of accounting for the effect of MDL on the accumulated amplification noise. Finally, in Sec. 6 we provide a description of the numerical procedure that was used to obtain the simulation results that are displayed throughout this paper. The derivation of all the reported analytical results is provided in the appendix.

2. Optical amplifier types for SDM and their impact on performance

We consider an SDM link consisting of multiple amplified spans where modes propagate in the strong coupling regime [15, 16]. Each span is modeled as consisting of a large number of statistically independent and identically distributed MDL elements, which, in the absence of any other knowledge, are assumed to be isotropic in the generalized multidimensional Stokes space [15]. The physical meaning of such isotropy is that the propagation modes are equivalent from the standpoint of MDL statistics. The gain and the amplification noise introduced by the amplifiers are assumed to be mode-independent. We note that this is not a limiting assumption, as an amplifier suffering from mode-dependent gain and noise is equivalent to an amplifier having perfectly isotropic gain and noise preceded or followed by an MDL element. For a consistent analysis of capacity, we need to account for the fact that MDL is frequency dependent, with the correlation bandwidth being inversely proportional to the link's modal dispersion (MD) [15, 17]. While the specific MD value may vary from link to link and is still lacking sufficient experimental characterization, the correlation bandwidth is certainly much narrower than the overall WDM band. In what follows we divide the WDM band into narrow sub-bands with frequency independent MDL. In other words, each sub-band represents an independent realization of a frequency-flat MIMO-SDM channel. For each sub-band the information capacity can be readily determined [1, 5], and the overall capacity follows from summing the capacities over the individual sub-bands. Note that the division into sub-bands is a standard way of evaluating the capacity on a frequency-varying channel.

We consider two possible schemes in which the inline amplifiers can operate, as illustrated in Fig. 1. In Scheme 1 the amplifiers restore the mode-averaged signal power over the entire

#225568 - $15.00 USD Received 24 Oct 2014; revised 2 Dec 2014; accepted 5 Dec 2014; published 28 Jan 2015
© 2015 OSA

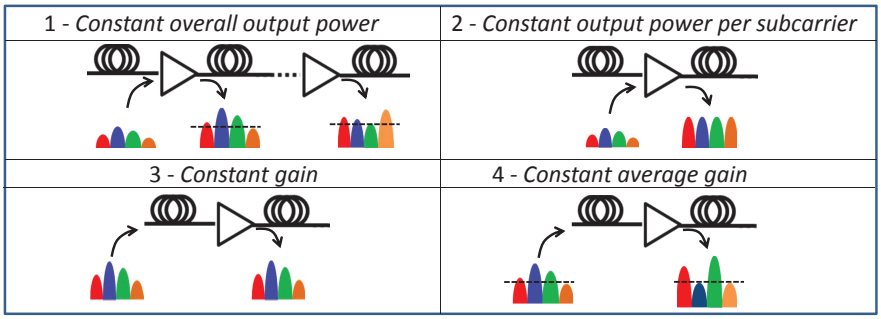

Fig. 1. Amplification schemes considered in the analysis. In Scheme 1 each amplifier restores the mode-averaged signal power over the entire band of frequencies. In Scheme 2 the mode-averaged signal power is restored separately for each sub-band. In Scheme 3 each amplifier restores the mode-averaged power of a sub-band to the value that it had at the input of the span. Scheme 4 operates in the same way as Scheme 3, except that it restores the mode-averaged signal power across the entire band of frequencies.

band of frequencies. In scheme 2 the mode-averaged signal power is restored separately for each sub-band, which makes Scheme 2 a frequency-resolved power equalization scheme. In order to reconcile the present study with that of [1], we also consider a third scheme which assumes equalization on a per sub-band basis, but applied separately on each span. Namely, each amplifier restores the mode-averaged power of each sub-band to the value that it had at the input of the span. For the sake of completeness, we also consider a fourth scheme, which operates similarly to Scheme 3, except that it restores the signal power across the entire band of frequencies to its value at the beginning of the span. If we denote by $\mathbf{M}_k$ the transfer matrix of the k-th span (including the k-th amplifier), and by $\mathbf{T}_k = \mathbf{M}_k\mathbf{M}_{k-1}\ldots\mathbf{M}_1$ the transfer matrix of the link between the transmitter and the end of the k-th span, the described schemes can be summarized as shown in Table 1, where $2N$ is the total number of transmitted modes, with the factor of 2 accounting for polarization. The angled brackets denote ensemble averaging, which, under the assumption of frequency ergodicity, is equivalent to frequency averaging over all sub-bands making up the full WDM band. This equivalence requires that the WDM band is sufficiently large relative to the spectral correlation of MDL. Although the accuracy of this assumption might be questionable in the very beginning of the link (where MD may still be small, and hence the correlation bandwidth may be large), it becomes more and more justified when the accumulated MD exceeds the inverse WDM bandwidth. In the limit of strong mode coupling within the individual spans, as we show in the appendix, Scheme 4 is rigorously equivalent to Scheme 1, in spite of the fact that the implementations of the two schemes are very different. For this reason we do not refer to Scheme 4 explicitly in what follows.

Table 1. Analytic description of the amplification schemes of Fig. 1.

Scheme 1: $\left\langle \mathrm{Tr}\left[\mathbf{T}_k^\dagger\mathbf{T}_k\right]\right\rangle = 2N$	Scheme 2: $\mathrm{Tr}\left[\mathbf{T}_k^\dagger\mathbf{T}_k\right] = 2N$
Scheme 3: $\mathrm{Tr}\left[\mathbf{M}_k^\dagger\mathbf{M}_k\right] = 2N$	Scheme 4: $\left\langle \mathrm{Tr}\left[\mathbf{M}_k^\dagger\mathbf{M}_k\right]\right\rangle = 2N$

Throughout the paper we use the formalism introduced in [5] where all the system consequences of MDL are captured by four quantities; the MDL vector $\vec{\Gamma}$, the noise coherency vector $\vec{\Gamma}'$, the mode averaged signal loss γ_0, and the mode averaged noise power γ_0'. However, unlike

#225568 - $15.00 USD Received 24 Oct 2014; revised 2 Dec 2014; accepted 5 Dec 2014; published 28 Jan 2015
© 2015 OSA

in [5], we define γ_0' as a unitless coefficient which similarly to γ_0 is unity in the absence of MDL. Thus the overall mode-averaged noise power (which was denoted by γ_0' in [5]) is now given by $P_n\gamma_0'$, where P_n is the sum of the noise powers generated per mode by the amplifiers. While the analytical results that we present here and derive in Sec. 7 are obtained for the case of distributed amplification, we show in what follows that they also hold in realistic system scenarios assuming lumped optical amplifiers. In the present analysis we quantify the impact of MDL on system capacity by means of the capacity loss per mode ℓ, which is defined as

$$\ell = \frac{C_{\text{ref}} - C}{2N}, \tag{1}$$

where C is the actual system capacity and where C_{ref} is the capacity of the MDL-free system that is assumed as a reference. The difference between this metric and the frequently encountered capacity ratio C/C_{ref} will be discussed in Sec. 3. Note that the choice of the reference system is important in assessing the impact of MDL. We assume that the reference system operates at an SNR of $S_{\text{ref}} = S_0 \frac{\langle\gamma_0\rangle}{\langle\gamma_0'\rangle}$, which is the value that one would obtain by measuring the ratio between the aggregate signal and noise powers averaged over time or frequency. Also, we assume that no channel state information is available at the transmitter, which hence excites the $2N$ modes with the same average power. The capacity of the reference system is in this case $C_{\text{ref}} = 2N\log_2(1+S_{\text{ref}})$. First, we argue that the average capacity loss due to MDL is the same for all the considered amplification schemes and it is given by

$$\langle\ell\rangle = \frac{\langle\Gamma^2\rangle}{3\log(2)}, \tag{2}$$

where Γ is the length of the MDL vector $\vec{\Gamma}$. The difference between the schemes is in the *fluctuations* of the capacity loss, which is characterized by the variance of ℓ, and consequently determines the system's outage behavior. As shown in the appendix, in the case of Scheme 1, where the amplifiers are set to reproduce the total mode-averaged output power in the WDM band, the variance of the MDL-induced capacity reduction is given by

$$\sigma_1^2 = \frac{\langle\ell\rangle^2}{20(4N^2-1)}. \tag{3}$$

For Scheme 2, where the amplifiers equalize the mode-averaged signal power separately for the individual sub-bands, the variance is given by

$$\sigma_2^2 = \left[22 - \frac{15(5\alpha_0 L - 6)}{\alpha_0^2 L^2}\right]\sigma_1^2, \tag{4}$$

where L is the overall fiber length and α_0 is the mode-averaged fiber loss coefficient. For long fiber links, Eq. (4) reduces to $\sigma_2^2 \simeq 22\sigma_1^2$. An equivalent expression for Scheme 3 could not be derived, and hence its performance will only be analyzed numerically in what follows.

An important consequence of Eqs. (3) and (4) is that in the regime of large mode counts the fluctuations of the capacity loss per mode become negligible, as can be seen from the fact that their standard deviation is proportional to $\sim \langle\ell\rangle/2N$. This observation suggests that in such a regime only a small margin needs to be allocated to prevent MDL-induced outages. Of course, as will be discussed later, the situation is significantly different in systems with low mode counts.

The different behaviors of the three schemes are compared in Fig. 2, where we plot the probability density function (PDF) and the complementary cumulative distribution function

#225568 - $15.00 USD Received 24 Oct 2014; revised 2 Dec 2014; accepted 5 Dec 2014; published 28 Jan 2015
© 2015 OSA

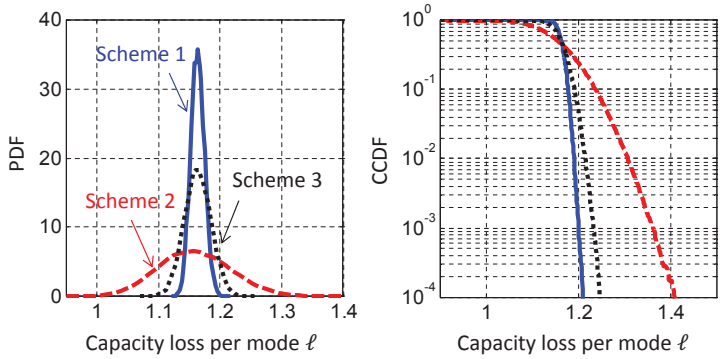

Fig. 2. The left panel shows the PDF of the MDL-induced capacity loss per mode ℓ for a system consisting of 20 amplified spans where $N = 10$ spatial modes are transmitted and for a link MDL of 24.6 dB (corresponding to about 5.5 dB per span). The right panel shows the corresponding complementary cumulative distribution function (CCDF), namely the probability of the capacity loss per mode ℓ exceeding the value on the abscissa.

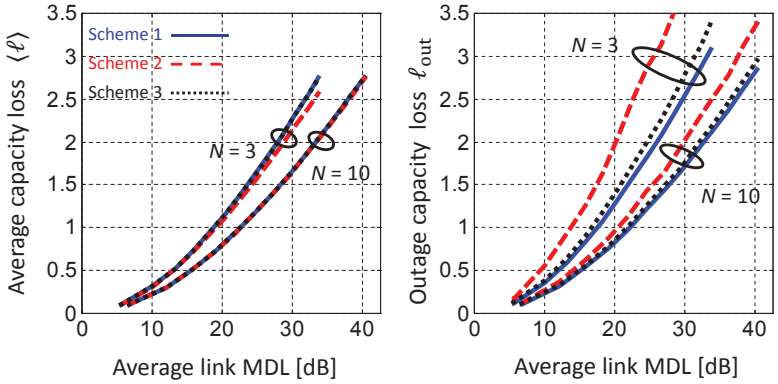

Fig. 3. The left panel shows the average capacity loss per mode as a function of the average link MDL in the limit of large SNR for amplification schemes 1, 2, and 3 of Fig. 1. The right panel shows the corresponding values of the outage capacity loss per mode. The results are shown for the cases of $N = 3$ and $N = 10$ spatial modes.

(CCDF) of ℓ, in the left and right panels, respectively, in the limit of large SNR [18]. These plots were produced for a system consisting of 20×100 km amplified spans of fiber supporting $N = 10$ spatial modes (this mode count is consistent with the situation of a weakly guiding fiber with normalized frequency $V \simeq 6$, where LP_{01}, LP_{11}, LP_{21}, LP_{02}, LP_{31}, and LP_{12} modes are guided). The mean MDL of the link was 24.6 dB (corresponding to $24.6/\sqrt{20} \simeq 5.5$ dB per span), and the details on how the simulations were conducted are provided in Section 6. As predicted by the theory, the average capacity loss per mode $\langle \ell \rangle$ is the same for the three schemes, but the widths of the distributions are notably different, with $\sigma_2/\sigma_1 \simeq 5.3$ and $\sigma_3/\sigma_1 \simeq 1.9$. The theoretically predicted ratio given by Eq. (4) is $\sigma_2/\sigma_1 = 4.7$. Given the large MDL value used in the simulation, the accuracy of the analytical result (derived in the limit of small to moderate MDL values) is quite impressive. The right panel of Fig. 2 can be used to extract the outage capacity loss per mode in the case where the MDL is approximately constant within the bandwidth of a WDM channel. For example, when setting the outage probability to the value

#225568 - $15.00 USD Received 24 Oct 2014; revised 2 Dec 2014; accepted 5 Dec 2014; published 28 Jan 2015
© 2015 OSA

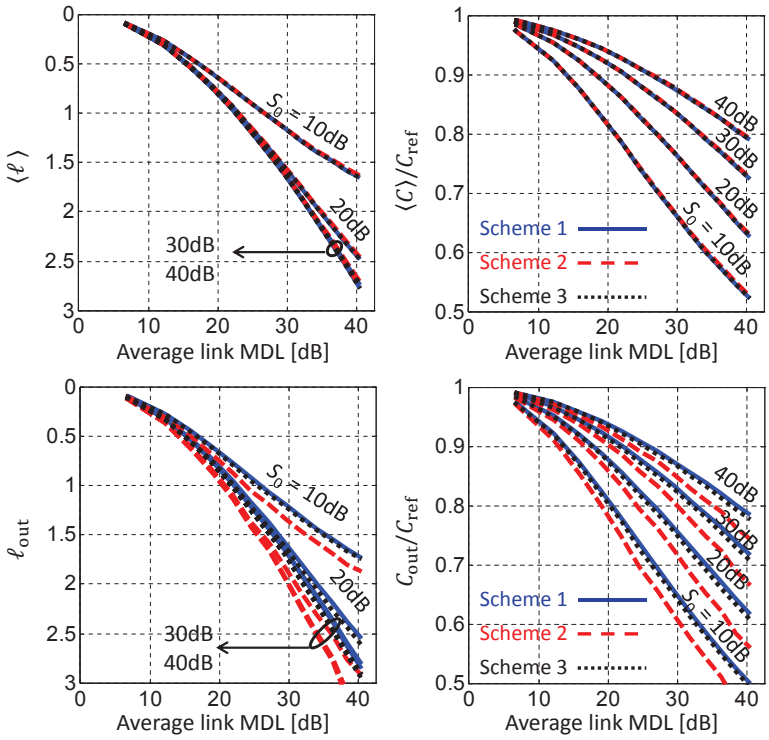

Fig. 4. The top left panel shows the average capacity loss per mode as a function of the average link MDL for SNR values of $S_0 = 10, 20, 30,$ and 40 dB. The top right panel shows the corresponding values of the average capacity ratio. The bottom left and right panels show the outage capacity loss per mode and the outage capacity ratio, respectively, versus the average link MDL for the same SNR values as in the top panels.

of 10^{-4}, the outage capacity loss per mode $\ell_{\rm out}$ for scheme 2 is 0.2 bits larger than in the case of scheme 1.

These points are further addressed in Fig. 3, where we plot the average and the outage values of the capacity loss per mode as a function of the mean MDL of the link, for the two cases of $N = 3$ and $N = 10$. The difference in the outage capacities between the amplification schemes is more evident in the case $N = 3$, and in general it decreases when the number of modes increases. In fact, the difference between the outage capacity values of any two schemes a and b, denoted by $\ell_{{\rm out},a}$ and $\ell_{{\rm out},b}$, is proportional to the difference between the corresponding standard deviations of the capacity loss per mode, σ_a and σ_b. In the case of Schemes 1 and 2 one can use Eqs. (3) and (4) to show that $\sigma_2 - \sigma_1 \propto \langle \ell \rangle / 2N$, which is inversely proportional to the number of modes, consistent with Fig. 3.

3. Capacity loss per mode vs. capacity ratio

In this section we discuss the role of quantifying the impact of MDL in terms of the capacity loss per mode $\ell = (C_{\rm ref} - C)/2N$, as opposed to the more frequently used capacity ratio $C/C_{\rm ref}$ [1–4, 6]. While both quantities are reliable figures of merit, the capacity loss per mode, in the relevant limit of high SNR, becomes independent of S_0 and reflects only the MDL parameters of the system, which makes this metric attractive. This point is illustrated in Fig. 4, where we

#225568 - $15.00 USD Received 24 Oct 2014; revised 2 Dec 2014; accepted 5 Dec 2014; published 28 Jan 2015
© 2015 OSA

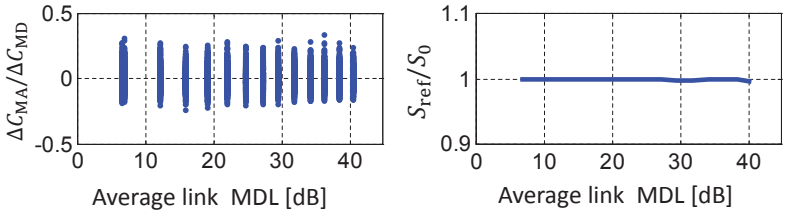

Fig. 5. The left panel shows the ratio between the second and the third terms of Eq. (5) in the form of a scatter plot versus the average link MDL. See text for details. The right panel shows the ratio between S_{ref} and S_0. Amplification scheme 1 has been assumed in both plots, but the same behavior has been observed for all amplification schemes.

plot the average capacity loss per mode in the top left panel and the average relative capacity in top right panel, versus the average link MDL. It is evident from the figure that the curves in the left panel become practically indistinguishable when S_0 exceeds 20 dB, whereas in the right panel the curves remain distinctively different. The curves are identical for all the considered amplification schemes. As shown in bottom panels of the same figure, when plotting the outage capacity loss per mode versus the average link MDL, a similar behavior is observed, namely the outage capacity loss per mode becomes independent of the SNR for large SNR values. However the outage capacity loss curves are different for the three amplification schemes.

4. Impact of specifying the SNR in MDL-impaired systems

The dependence of the MDL-induced penalty on the amplification scheme shown in Fig. 3 exemplifies the sensitivity of the MDL-induced capacity reduction to certain details of system operation. We show in what follows that this sensitivity also extends to two system modeling aspects. These are the definition of the MDL-free reference system, which is discussed in this section, and the modeling of the amplification noise, which is the subject of the next section.

A subtle aspect of MDL is that, when looking at the system information capacity, the randomness of mode-averaged signal and noise powers is as important as the fact that the individual eigenmodes are characterized by random and different attenuations. In our formalism, this is equivalent to claiming that the randomness of γ_0 and γ_0' is as important as the randomness of $\vec{\Gamma}$ and $\vec{\Gamma}'$. In order to illustrate this, we recall the expression for the system information capacity which has been derived in the regime of large SNR in [5]

$$C = 2N\log_2(S_0) + \underbrace{2N\log_2\left(\frac{\gamma_0}{\gamma_0'}\right)}_{\Delta C_{\mathrm{MA}}} + \underbrace{\log_2\left\{\det\left[\left(\mathbf{I}+\vec{\Gamma}\cdot\vec{\Lambda}\right)\left(\mathbf{I}+\vec{\Gamma}'\cdot\vec{\Lambda}\right)^{-1}\right]\right\}}_{\Delta C_{\mathrm{MD}}}, \tag{5}$$

where the only previously undefined quantity is $\vec{\Lambda}$, which is an extension of the Pauli matrix vector known in the context of PMD studies [19], introduced to MIMO-SDM systems in [15]. The first term on the right hand side of Eq. (5) is the capacity of the system in the absence of MDL. The second term represents the capacity penalty caused by the fluctuations of the mode-averaged signal and noise powers and we therefore denote it by ΔC_{MA}, where the subscript MA stands for "mode-averaged." The third term is the capacity penalty caused directly by the existence of differential losses and gains, which are described by the MDL vector $\vec{\Gamma}$ and by the noise coherency vector $\vec{\Gamma}'$, and we denote this term by ΔC_{MD}, where the subscript MD stands for "mode-dependent." In the left panel of Fig. 5 we show the ratio $\Delta C_{\mathrm{MA}}/\Delta C_{\mathrm{MD}}$ in the form of a scatter plot in a range of average link MDL values. It can be seen from the figure that

#225568 - $15.00 USD Received 24 Oct 2014; revised 2 Dec 2014; accepted 5 Dec 2014; published 28 Jan 2015
© 2015 OSA

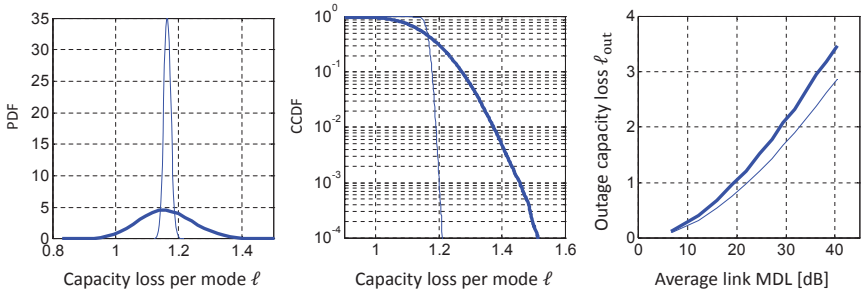

Fig. 6. The left panel shows by thick curve the PDF of the capacity loss per mode ℓ for the same system as in Fig. 2, which is obtained by assuming amplification scheme 1 and by setting the reference SNR to $S'_{\rm ref} = S_0 \frac{\gamma_0}{\gamma'_0}$. The thin curve is taken from Fig. 2, and is shown for comparison. The center panel shows the corresponding CCDFs. The right panel shows the outage capacity loss in the two cases for increasing values of the average link MDL.

the magnitude of $\Delta C_{\rm MA}$ is non-negligible as it reaches values as large as one quarter of the mode-dependent term $\Delta C_{\rm MD}$.

In order to see why this is the case, we recall that the end-to-end MDL of a link is the result of many local perturbations such as imperfect splices, micro-bends, etc. These make the attenuation coefficients of the *local* eigenmodes random quantities, which can be characterized by a standard deviation σ_α. In the regime of small MDL, $\vec{\Gamma}$ and $\vec{\Gamma}'$ have been shown in [5] to scale with σ_α, whereas we show in the appendix that $\gamma_0 = 1+\Delta\gamma_0$ and $\gamma'_0 = 1+\Delta\gamma'_0$, where $\Delta\gamma_0$ and $\Delta\gamma'_0$ scale with σ_α^2. In this regime Eq. (5) reduces to

$$C = 2N\log_2(S_0) + \frac{2N}{\ln(2)}\left(\Delta\gamma_0 - \Delta\gamma'_0 - \frac{\Gamma^2 - \Gamma'^2}{2}\right), \tag{6}$$

which depends linearly on $\Delta\gamma_0$ and $\Delta\gamma'_0$, and quadratically on Γ and Γ', so that all of the contributions scale with σ_α^2, and they are therefore of similar importance. This situation is in contrast with MDL studies where the preferred metric is the deterioration in the worst channel's signal-to noise-ratio, or in the average bit-error-rate (BER) [9,11]. There the relevant quantities depend linearly on all four parameters $\Delta\gamma_0$, $\Delta\gamma'_0$, $\vec{\Gamma}$, and $\vec{\Gamma}'$, and therefore the contribution of $\Delta\gamma_0$ and $\Delta\gamma'_0$ is negligible. Indeed it has been shown in [9] that the dependence of the BER on the fluctuations of the ratio between the mode-averaged signal and noise powers becomes noticeable only in the regime of very large MDL values.

The above discussion is closely related to the question of which reference system one should use to quantify the effect of MDL on capacity. In one case, one may opt to choose a reference system operating at an SNR value of $S_0 = P_s/P_n$, which is the SNR that one would measure if it were possible to remove all of the local MDL sources [3]. Obviously this approach is not practical since the only measurable quantities at the system output are $\gamma_0 P_s$ and $\gamma'_0 P_n$. Since these are random quantities, an acceptable definition would be that the reference SNR is set to $S_{\rm ref} = S_0 \frac{\langle\gamma_0\rangle}{\langle\gamma'_0\rangle}$, ad we assumed in this work. The ensemble averaging involved in the definition of $S_{\rm ref}$ can be approximated by averaging the aggregate signal and noise powers either in time or in frequency. On the other hand, if proper averaging cannot be performed (when the timescale of MDL dynamics is too slow [20], or if one does not have access to a sufficiently broad spectrum in an operating system), one can only resort to defining the reference SNR as $S'_{\rm ref} = S_0 \frac{\gamma_0}{\gamma'_0}$, which is what was assumed in [5]. It is also customary to set the SNR to $S'_{\rm ref}$ when evaluating the relation between SNR and BER in simulated systems [9].

#225568 - $15.00 USD Received 24 Oct 2014; revised 2 Dec 2014; accepted 5 Dec 2014; published 28 Jan 2015
© 2015 OSA

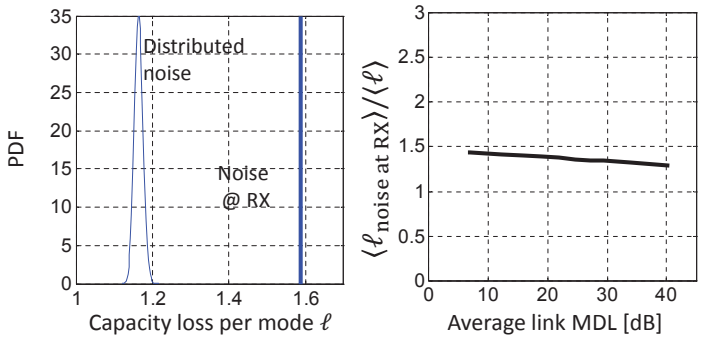

Fig. 7. The left panel shows by thick curve the PDF of the capacity loss per mode ℓ for the same system as in Fig. 2, which is obtained for amplification scheme 1 by assuming that spatially isotropic noise is loaded at the receiver, rather than at the inline amplifier sites as it should be. The thin curve is the corresponding PDF taken from Fig. 2. The right panel shows the ratio between the average capacity losses per mode obtained for the two noise models versus the average link MDL.

Interestingly, in a relevant range of MDL values, S_{ref} turns out to be practically identical to S_0, as can be seen in the right panel of Fig. 5, where we plot the ratio $\frac{\langle \gamma_0 \rangle}{\langle \gamma_0' \rangle}$ as a function of the average link MDL. The situation changes drastically when setting the reference SNR to S'_{ref}, as we illustrate in Fig. 6. In the left and center panels of the figure we compare the PDF and the CCDF obtained for amplification scheme 1 by setting the reference SNR to S'_{ref} with the corresponding distributions of Fig. 2, which are shown by thin curves. While the average capacity loss is the same for the two choices of reference system, as we demonstrate in the appendix, the variance of the capacity loss per mode in this case is $\sigma_1'^2 = 55\sigma_1^2$, consistent with the broadening of the distributions seen in the figure, and with the corresponding increase in outage capacity loss per mode (the computed ratio between $\sigma_1'^2$ and σ_1^2 is approximately 62). A direct comparison of the outage capacity loss obtained for the two settings of the reference SNR (assuming an outage probability of 10^{-4}) is presented in the right panel. Finally, we note that when setting the reference SNR to S'_{ref} the MDL impact on system performance is practically unaffected by the assumed amplification scheme.

5. Noise loading

Another important and often overlooked aspect of modeling MDL has to do with whether or not the effect of MDL on the amplification noise is accounted for – an issue that has been addressed to some extent in [1, 5, 21]. In all of the above results, noise was assumed to be added to the propagating signal distributed at each amplification site. If instead spatially isotropic noise is assumed to be added at the receiver, as in [2, 3], the average capacity loss per mode ℓ increases by a factor of up to 3/2 relative to the actual value.

In Fig. 7 we illustrate the importance of correctly accounting for the effect of MDL on the noise spatial coherency, where the amplifiers are operated according to scheme 1. Here, the average capacity loss when the noise is added at the end is significantly larger than the actual average capacity loss. This can clearly be seen in the left panel, which shows the PDF of capacity loss ℓ, with noise properly distributed (thin curve, identical to the corresponding curve in Fig. 2) and when spatially isotropic noise is added at the receiver (thick curve). Note that when the noise is added at the receiver, the PDF of the capacity loss approaches a delta function (we show in the appendix that the variance of ℓ reduces to zero to first order in σ_α^2). The right panel

#225568 - $15.00 USD Received 24 Oct 2014; revised 2 Dec 2014; accepted 5 Dec 2014; published 28 Jan 2015
© 2015 OSA

of Fig. 7 shows the ratio between the average capacity loss calculated when assuming noise loading at the receiver and the actual capacity versus the average link MDL. The plot shows that the ratio of 1.5 derived in the regime of small MDL remains approximately valid for large MDL values.

6. Numerical simulations

In this section we provide the details concerning the simulations that have been performed in the context of this paper and whose results are displayed in Figs. 2-7. In all our simulations we assumed the regime of strong mode coupling.

The simulated system contained $N_s = 20$ amplified spans, with every span constructed of $M = 100$ MDL elements, each characterized by a local MDL vector $\vec{\alpha}_{k,j}$. This choice ensures that each MDL element contributes incrementally to the overall MDL, consistently with the theory. Cases in which few MDL elements are responsible for dominant contributions to the overall MDL are not treated in this paper. We verified that varying the number of spans within a relevant range of values does not affect the results. Each vector $\vec{\alpha}_{k,j}$ is independently drawn at random from an isotropic Gaussian distribution with the value of $\langle \alpha^2 \rangle \equiv \langle |\vec{\alpha}_{k,j}|^2 \rangle$ being a parameter. The transfer matrix $\mathbf{A}_{k,j}$ of the j-th MDL element in the k-th span is first set to the matrix $\exp(\frac{1}{2}\vec{\alpha}_{k,j} \cdot \vec{\Lambda})$ and then normalized such that the average trace of $\mathbf{A}_{k,j}\mathbf{A}_{k,j}^{\dagger}$ is equal to $2N$. In the limit where the magnitude of the local MDL vector $\vec{\alpha}_{k,j}$ is small, it can be shown that this normalization is equivalent to setting $\mathbf{A}_{k,j} = \exp(-\frac{1}{4}\langle \alpha^2 \rangle) \exp(\frac{1}{2}\vec{\alpha}_{k,j} \cdot \vec{\Lambda})$. The transfer matrix of the k-th span is $\mathbf{M}_k = \sqrt{G_k} \exp\left(-\frac{1}{2}\frac{\alpha_0 L}{N_s}\right) \mathbf{A}_{k,M}\mathbf{A}_{k,M-1}\ldots\mathbf{A}_{k,1}$, where G_k is the gain of the k-th amplifier. The transfer matrix describing propagation from the link input to the end of the h-th span is $\mathbf{T}_h = \mathbf{M}_h\mathbf{M}_{h-1}\ldots\mathbf{M}_1$.

When simulating amplification scheme 2, G_k is set so that the trace of $\mathbf{T}_h\mathbf{T}_h^{\dagger} = 2N$ for all values of h. Similarly, in the case of scheme 3, G_k is set so that the trace of $\mathbf{M}_k\mathbf{M}_k^{\dagger} = 2N$ for all values of k. The case of scheme 1 is somewhat less straightforward to simulate, as it requires the computation of ensemble averages prior to setting the individual gain values. We show in the appendix that in the limit where every span contains a large number of small MDL contributions, this is equivalent to setting $G_k = \exp\left(\frac{\alpha_0 L}{N_s}\right)$.

The noise coherency matrix is computed as $\mathbf{Q} = (G_{N_s} - 1)\mathbf{I} + \sum_{k=2}^{N_s}(G_{k-1} - 1)\mathbf{F}_k\mathbf{F}_k^{\dagger}$, where $\mathbf{F}_k = \mathbf{M}_{N_s}\ldots\mathbf{M}_k$ is the transfer function of the last $(N_s - k + 1)$ spans, and where we used the fact that the power of the amplification noise generated by an amplifier with gain G is proportional to $G - 1$. In all numerical examples we assumed that the mode-averaged loss coefficient is $\alpha_0 = 0.0461$ Np/km, corresponding to 0.2 dB/km.

We verified that simulations of the same system based on the numerical method presented in [1] yield results which are in full agreement with those presented here.

7. Conclusions

Mode-dependent loss is expected to be a major issue in MIMO-SDM systems. In this paper we have shown that the accurate assessment of its impact on system performance requires carefully addressing a number of aspects that have received little attention in previous studies.

To quantify the impact of MDL we assumed as a metric the capacity loss per mode, which is defined as $\ell = (C_{\text{ref}} - C_0)/2N$, where C is the capacity of the MDL-impaired system, C_{ref} is the capacity of an MDL-free system which is assumed as a reference, and $2N$ is the number of modes, including polarizations. We showed that the average value of ℓ is independent of how the inline optical amplifiers are operated. In contrast, its fluctuations - and hence the corresponding outage values - are proportional to $\langle \ell \rangle / 2N$, with the proportionality coefficient ranging between

#225568 - $15.00 USD Received 24 Oct 2014; revised 2 Dec 2014; accepted 5 Dec 2014; published 28 Jan 2015
© 2015 OSA

$1/\sqrt{20}$ and $\sqrt{55}/\sqrt{20}$, depending on the amplification scheme and on the assumptions that are made on the MDL-free reference system. Since the size of these fluctuations reduces with the number of modes, the impact of the amplification scheme is more significant in systems with low mode counts. In the regime of large mode counts the capacity loss fluctuations become very small and, as a result, no significant margin is to be allocated in this case for MDL-induced outages.

We also discussed the choice of metrics to quantify the impact of MDL on system performance. We showed that the capacity loss per mode ℓ, compared to the frequently used capacity ratio C/C_{ref}, has the advantage of depending very weakly on the SNR value in the regime of large SNR.

The sensitivity of the capacity loss on the amplification scheme arises from the MDL-induced fluctuations of the mode-averaged signal and noise powers. We showed that the same fluctuations are responsible for the dependence of ℓ on the choice of the MDL-free system that is assumed as a reference to evaluate the MDL-induced capacity reduction.

Finally, we quantified the error that is incurred when neglecting the effect of MDL on amplification noise. The capacity loss per mode is approximately 50% larger if one assumes, as is sometimes done in MDL studies, that isotropic noise is added to the signal at the receiver, as compared to the case where ASE noise is properly assumed to be loaded at each inline amplifier.

Appendix: Analysis

The information capacity of an SDM system where $2N$ modes (including polarizations) are transmitted, in the absence of channel state information at the transmitter, is given by

$$C = \log_2\left[\det\left(\mathbf{I} + S_0\mathbf{Q}^{-1/2}\mathbf{T}\mathbf{T}^{\dagger}\mathbf{Q}^{-1/2}\right)\right], \tag{7}$$

where $S_0 = P_s/P_n$ is the SNR that would be measured in the absence of MDL, $\mathbf{T}$ is the $2N \times 2N$ channel transfer matrix, and $\mathbf{I}$ denotes the identity. The matrix $\mathbf{Q}$ is the noise space coherency matrix normalized to the MDL-free noise power P_n, such that its trace in the absence of MDL is equal to $2N$. We recall that the matrices $\mathbf{T}\mathbf{T}^{\dagger}$ and $\mathbf{Q}$ are Hermitian, and hence they can be expressed as

$$\mathbf{T}\mathbf{T}^{\dagger} = \gamma_0\left(\mathbf{I} + \vec{\Gamma}\cdot\vec{\Lambda}\right), \ \mathbf{Q} = \gamma_0'\left(\mathbf{I} + \vec{\Gamma}'\cdot\vec{\Lambda}\right), \tag{8}$$

where γ_0 is the mode-averaged channel attenuation, $\vec{\Gamma}$ is the MDL vector, γ_0' is the mode-averaged noise power, and $\vec{\Gamma}'$ is the noise coherency vector. For an extensive description of the formalism used in this Appendix, the reader is referred to [5]. In the limit of large signal-to-noise ratio and small MDL, Eq. (7) can be approximated by

$$\frac{C}{2N} \simeq \log_2\left(S_0\frac{\gamma_0}{\gamma_0'}\right) + \frac{\Gamma'^2 - \Gamma^2}{2\ln(2)} \simeq \log_2(S_0) - \frac{1}{2}\log_2\left(\frac{\gamma_0'^2 - \gamma'^2}{\gamma_0^2 - \gamma^2}\right), \tag{9}$$

where γ and γ' denote the lengths of the vectors $\vec{\gamma} = \gamma_0\vec{\Gamma}$ and $\vec{\gamma}' = \gamma_0'\vec{\Gamma}'$, respectively, and where the second equality on the right-hand side of Eq. (9) is correct to first order in Γ^2 and Γ'^2. After expanding the logarithm, the above yields

$$\frac{C}{2N} = \log_2(S_0) - \frac{1}{2\log(2)}\left(\frac{\gamma_0'^2 - \gamma'^2}{\gamma_0^2 - \gamma^2} - 1\right). \tag{10}$$

This allows us to calculate the MDL capacity loss per mode ℓ, which in the limit of large SNR reduces to

$$\ell = \log_2(S_{\text{ref}}) - \frac{C}{2N} = \log_2\left(\frac{\langle\gamma_0'\rangle}{\langle\gamma_0\rangle}\right) + \frac{1}{2\log(2)}\left(\frac{\gamma_0'^2 - \gamma'^2}{\gamma_0^2 - \gamma^2} - 1\right). \tag{11}$$

#225568 - $15.00 USD Received 24 Oct 2014; revised 2 Dec 2014; accepted 5 Dec 2014; published 28 Jan 2015
© 2015 OSA

We now derive evolution equations for $\gamma_0^2-\gamma^2$ and for $\gamma_0'^2-\gamma'^2$, as well as an expression for $\langle\gamma_0\rangle/\langle\gamma_0'\rangle$. The equation for $\gamma_0^2-\gamma^2$ follows from the equations for γ_0 and $\vec{\gamma}$ in [5], in which we neglect terms that are of second order in MDL in the equation for $\vec{\gamma}$ and of third order in MDL in the equation for γ_0 (as required for consistency since Eq. (11) involves the first power of γ_0, but only the second power of γ),

$$\frac{\mathrm{d}\gamma_0}{\mathrm{d}z}=-(\alpha_0+\alpha'-g)\gamma_0-\vec{\alpha}\cdot\vec{\gamma},\qquad \frac{\mathrm{d}\vec{\gamma}}{\mathrm{d}z}=-(\alpha_0+\alpha'-g)\vec{\gamma}-\gamma_0\vec{\alpha}. \tag{12}$$

Compared to the same equations derived in [5], Eqs. (12) contain an extra term characterized by the mode-averaged loss coefficient α'. As will become evident in what follows, this term was introduced to ensure that $\langle\gamma_0(z)\rangle$ which represents the ensemble average of the mode averaged gain, is equal to $\exp[(g-\alpha_0)z]$, as would be the case in an MDL-free system. We now approximate the local MDL vector $\vec{\alpha}$ as a white Gaussian noise process, in which case $\vec{\alpha}\mathrm{d}z$ is an increment $\mathrm{d}\vec{W}$ of a three-dimensional Wiener process and its variance $\mathrm{d}W^2=\sigma_\alpha^2\mathrm{d}z$ represents the magnitude of the local MDL along the system. Rewriting Eqs. (12) in the standard Ito form [22] yields

$$\mathrm{d}\gamma_0 = -\left(\alpha_0+\alpha'-\frac{\sigma_\alpha^2}{2}-g\right)\gamma_0\mathrm{d}z-\mathrm{d}\vec{W}\cdot\vec{\gamma}, \tag{13}$$

$$\mathrm{d}\vec{\gamma} = -\left(\alpha_0+\alpha'-\frac{\sigma_\alpha^2}{2}-g\right)\vec{\gamma}\mathrm{d}z-\gamma_0\mathrm{d}\vec{W}, \tag{14}$$

from which it is evident that in order to achieve its goal α' needs to be set to $\alpha'=\sigma_\alpha^2/2$. Substituting this value in Eqs. (13) and (14), conveniently yields

$$\mathrm{d}\gamma_0=-(\alpha_0-g)\gamma_0\mathrm{d}z-\mathrm{d}\vec{W}\cdot\vec{\gamma},\qquad \mathrm{d}\vec{\gamma}=-(\alpha_0-g)\vec{\gamma}\mathrm{d}z-\gamma_0\mathrm{d}\vec{W}. \tag{15}$$

The above equations can be used to obtain

$$\frac{\mathrm{d}(\gamma_0^2-\gamma^2)}{\mathrm{d}z}=-2\left(\alpha_0-g\right)\left(\gamma_0^2-\gamma^2\right)-\sigma_\alpha^2\gamma_0^2,. \tag{16}$$

Since $\sigma_\alpha^2\gamma^2\simeq 0$ to first order in σ_α^2, the term $\sigma_\alpha^2\gamma_0^2$ can be replaced with $\sigma_\alpha^2\left(\gamma_0^2-\gamma^2\right)$, and the solution of the resulting equation is

$$\gamma_0^2-\gamma^2=\exp\left\{-2I(0,z)-\sigma_\alpha^2 z\right\}, \tag{17}$$

where we defined $I(z_1,z_2)=\int_{z_1}^{z_2}(\alpha_0-g)\mathrm{d}z$, and where we used the initial conditions $\gamma(0)=0$ and $\gamma_0(0)=1$. Using the same procedure, the equations for noise parameters γ_0' and $\vec{\gamma}'$ that were introduced in [5] assume the form

$$\mathrm{d}\gamma_0'=-(\alpha_0-g)\gamma_0'\mathrm{d}z-\mathrm{d}\vec{W}\cdot\vec{\gamma}'+\frac{g}{\alpha_0 L}\mathrm{d}z,\qquad \mathrm{d}\vec{\gamma}'=-(\alpha_0-g)\vec{\gamma}'\mathrm{d}z-\gamma_0'\mathrm{d}\vec{W}, \tag{18}$$

and their solution with initial condition $\gamma'(0)=\gamma_0'(0)=0$ is given by

$$\gamma_0'^2-\gamma'^2=\frac{2}{\alpha_0 L}\int_0^L \mathrm{d}z' g(z')\gamma_0'(z')\exp\left\{-2I(z',z)-\sigma^2(z-z')\right\}. \tag{19}$$

Using Eqs. (17) and (19) the capacity loss per mode can be expressed as

$$\ell=\log_2\left(\frac{\langle\gamma_0'\rangle}{\langle\gamma_0\rangle}\right)+\frac{1}{2\ln(2)}\left[\frac{2}{\alpha_0 L}\int_0^L \mathrm{d}z' g(z')\gamma_0'(z')\exp\left\{2I(0,z')+\sigma^2 z'\right\}-1\right], \tag{20}$$

#225568 - $15.00 USD Received 24 Oct 2014; revised 2 Dec 2014; accepted 5 Dec 2014; published 28 Jan 2015
© 2015 OSA

where γ_0' is the solution of the first of Eqs. (18),

$$\gamma_0' = \int_0^L \exp\left\{-I(z',z)\right\}\left[-\mathrm{d}\vec{W}_{z'}\cdot\vec{\gamma}'(z') + \frac{g(z')}{\alpha_0 L}\mathrm{d}z'\right]. \tag{21}$$

The expression for $\vec{\gamma}'(z')$ is obtained by solving the second of Eqs. (18),

$$\vec{\gamma}' = -\int_0^L \exp\left\{-I(z',z)\right\}\gamma_0'(z')\mathrm{d}\vec{W}_{z'}, \tag{22}$$

where, to first order in σ_α^2 we approximate γ_0' with its zeroth order expression $\gamma_0' = z/L$, obtained from the first of Eqs. (18) by setting $g = \alpha_0$ in the absence of MDL.

In what follows we assume that the quantity $\alpha_0 - g$, and hence I, is first order in σ_α^2. We will verify that for amplification schemes 1 and 2 this is indeed the case. Note that this is also consistent with the fact that the link net gain is to be close to one (in the absence of MDL we assume that this is exactly one). Under this assumption Eqs. (22) and (21) reduce to

$$\vec{\gamma}' = -\frac{1}{L}\int_0^z z'\mathrm{d}\vec{W}_{z'}, \quad \gamma_0' = \frac{z}{L} + \frac{1}{L}\int_0^z \mathrm{d}\vec{W}_{z'}\cdot\int_0^{z'} z''\mathrm{d}\vec{W}_{z''} - \frac{1}{L}\int_0^z I(z',z)\mathrm{d}z' - \frac{1}{\alpha_0 L}I(0,z), \tag{23}$$

and, after some algebra involving integration by parts, as well as the equations $\alpha_0 - g = -\mathrm{d}I(z',z)/\mathrm{d}z'$ and $I(0,z') + I(z',z) = I(0,z)$, the expression for ℓ becomes

$$\ln(2)\ell = \ln\left(\frac{\langle\gamma_0'\rangle}{\langle\gamma_0\rangle}\right) + \frac{\sigma_\alpha^2 L}{3} + \frac{1}{L^2}\int_0^L (L-z')\int_0^{z'} z''\mathrm{d}\vec{W}_{z''}\cdot\mathrm{d}\vec{W}_{z'} + \frac{1}{L}\int_0^L I(0,z')\mathrm{d}z' - \frac{I(0,L)}{\alpha_0 L}, \tag{24}$$

where the last term accounts for the noise power dependence on z caused by gain non-uniformity along the link.

We are left with the calculation of $\langle\gamma_0'\rangle$ and $\langle\gamma_0\rangle$. For a given amplification scheme, the value of $\langle\gamma_0'\rangle$ can be evaluated by averaging the second of Eqs. (23), which involves evaluating the ensemble average of $I(z',z)$. This task can only be accomplished by assuming some amplification strategy. Finally, we can evaluate $\langle\gamma_0\rangle$ using for γ_0 the following expression, which, along with that of $\vec{\gamma}$, is obtained through a procedure similar to the one followed in the derivation of Eqs. (23),

$$\vec{\gamma} = -\int_0^z \mathrm{d}\vec{W}_{z'} \qquad \gamma_0 = 1 - I(0,z) + \int_0^z\int_0^{z'} \mathrm{d}\vec{W}_{z'}\cdot\mathrm{d}\vec{W}_{z''}. \tag{25}$$

In what follows we specialize the analysis to the cases of Scheme 1 and Scheme 2.

Amplification scheme 1

In our formalism the operation of Scheme 1 corresponds to enforcing the condition $\langle\mathrm{d}\gamma_0(z)\rangle = 0$ in the first of Eqs. (16), which is obtained by setting $g = \alpha_0$. In this case $I = 0$ and $\langle\gamma_0'\rangle = z/L$, $\langle\gamma_0\rangle = 1$, and the capacity loss per mode reduces to

$$\ln(2)\ell = \frac{\sigma_\alpha^2 L}{3} + \frac{1}{L^2}\int_0^L (L-z')\int_0^{z'} z''\mathrm{d}\vec{W}_{z''}\cdot\mathrm{d}\vec{W}_{z'}. \tag{26}$$

The second term on the right-hand side of Eq. (26) averages to zero because in Ito's interpretation, the increments $\mathrm{d}\vec{W}_{z'}$ and $\mathrm{d}\vec{W}_{z''}$ never overlap [22], and hence the average capacity loss per mode is

$$\langle\ell\rangle = \frac{\sigma_\alpha^2 L}{3\ln(2)}. \tag{27}$$

#225568 - $15.00 USD Received 24 Oct 2014; revised 2 Dec 2014; accepted 5 Dec 2014; published 28 Jan 2015
© 2015 OSA

The fluctuations of the capacity loss per mode are given by

$$\sigma_1^2 = \left\langle \left[\frac{1}{L^2 \ln(2)} \int_0^L (L-z') \int_0^{z'} z'' \mathrm{d}\vec{W}_{z''} \cdot \mathrm{d}\vec{W}_{z'} \right]^2 \right\rangle. \tag{28}$$

After some algebra, one can find the following equality,

$$\left\langle \left[\int_0^L (L-z') \int_0^{z'} [z'' + f(z')] \mathrm{d}\vec{W}_{z''} \cdot \mathrm{d}\vec{W}_{z'} \right]^2 \right\rangle = \frac{\sigma_\alpha^4}{4N^2-1} \int_0^L (L-z')^2 \frac{[z'+f(z')]^3 - f^3(z')}{3} \mathrm{d}z' \tag{29}$$

which, for $f(z') = 0$ can be used to obtain the desired result,

$$\sigma_1^2 = \frac{\sigma_\alpha^4 L^2}{\ln^2(2) 180\,(4N^2-1)}. \tag{30}$$

In the derivation of (29) we used the properties

$$\langle \mathrm{d}W_{z_1,i} \mathrm{d}W_{z_2,j} \rangle = D^{-1} \sigma_\alpha^2 \delta_{i,j} \delta(z_1 - z_2) \mathrm{d}z_1 \mathrm{d}z_2 \tag{31}$$

$$\begin{aligned} \langle \mathrm{d}\vec{W}_{z_1} \cdot \mathrm{d}\vec{W}_{z_2} \mathrm{d}\vec{W}_{z_3} \cdot \mathrm{d}\vec{W}_{z_4} \rangle &= \sum_{i,j} \langle \mathrm{d}W_{z_1,i} \mathrm{d}W_{z_2,i} \mathrm{d}W_{z_3,j} \mathrm{d}W_{z_4,j} \rangle \\ &= \sigma_\alpha^4 \delta(z_1 - z_2) \delta(z_3 - z_4) \mathrm{d}z_1 \mathrm{d}z_2 \mathrm{d}z_3 \mathrm{d}z_4 \\ &\quad + D^{-1} \sigma_\alpha^4 \delta(z_1 - z_3) \delta(z_2 - z_4) \mathrm{d}z_1 \mathrm{d}z_2 \mathrm{d}z_3 \mathrm{d}z_4 \\ &\quad + D^{-1} \sigma_\alpha^4 \delta(z_1 - z_4) \delta(z_2 - z_3) \mathrm{d}z_1 \mathrm{d}z_2 \mathrm{d}z_3 \mathrm{d}z_4. \end{aligned} \tag{32}$$

Note that in the case of lumped amplification ($g = 0$) the first of Eqs. (15) yields $\langle \gamma_0(z + L_s) \rangle = \gamma_0(z) \exp(-\alpha_0 L_s)$. For this reason, in the simulations of Scheme 1 the gain of each amplifier was set to $G_k = \exp(\alpha_0 L_s)$, so that $\langle \gamma_0 \rangle = 1$ at the end of each amplified span of length L_s.

7.0.1. Equivalence between Scheme 1 and Scheme 4

We express the matrix $\mathbf{T}_k^\dagger \mathbf{T}_k$ of Table 1 as $\mathbf{T}_k^\dagger \mathbf{T}_k = t_k \mathbf{I} + \vec{\Gamma}_k \cdot \vec{\Lambda}$, where $t_k = \mathrm{Tr}\left[\mathbf{T}_{k-1}^\dagger \mathbf{T}_{k-1} \right] / 2N$ and $\vec{\Gamma}_k$ are the mode-averaged loss and the MDL vector of the k-th span, respectively. This gives $\mathbf{M}_k^\dagger \mathbf{M}_k = \mathbf{M}_{k-1}^\dagger \mathbf{T}_k^\dagger \mathbf{T}_k \mathbf{M}_{k-1} = t_k \mathbf{M}_{k-1}^\dagger \mathbf{M}_{k-1} + \mathbf{M}_{k-1}^\dagger (\vec{\Gamma}_k \cdot \vec{\Lambda}) \mathbf{M}_{k-1}$. By averaging the two sides of this equation and taking their traces, we obtain $\langle \mathrm{Tr}\left[\mathbf{M}_k^\dagger \mathbf{M}_k \right] \rangle = \frac{\langle \mathrm{Tr}\left[\mathbf{T}_{k-1}^\dagger \mathbf{T}_{k-1} \right] \rangle}{2N} \langle \mathrm{Tr}\left[\mathbf{M}_{k-1}^\dagger \mathbf{M}_{k-1} \right] \rangle$, where we used the fact that different spans are statistically independent in terms of MDL, and in the strong coupling regime within each span $\langle \vec{\Gamma}_n \rangle = 0$ [5]. The derived equality implies that $\langle \mathrm{Tr}\left[\mathbf{M}_k^\dagger \mathbf{M}_k \right] \rangle = 2N$ if and only if $\langle \mathrm{Tr}\left[\mathbf{T}_k^\dagger \mathbf{T}_k \right] \rangle = 2N$, which proves the equivalence between the two schemes.

Amplification scheme 2

In our formalism the operation of Scheme 2 corresponds to enforcing the condition $\mathrm{d}\gamma_0 = 0$ in the first of Eqs. (16). This gives

$$I(0,z) = \int_0^z \mathrm{d}\vec{W}_{z'} \cdot \int_0^{z'} \mathrm{d}\vec{W}_{z''}. \tag{33}$$

In this case $\langle I \rangle = 0$, and hence $\langle \gamma_0' \rangle = z/L$, $\langle \gamma_0 \rangle = 1$, and the capacity loss per mode becomes

$$\ln(2)\ell = \frac{\sigma^2 L}{3} + \frac{1}{L^2} \int_0^L (L-z') \int_0^{z'} \left[z'' + L - \frac{L}{\alpha_0 (L-z')} \right] \mathrm{d}\vec{W}_{z''} \cdot \mathrm{d}\vec{W}_{z'} \tag{34}$$

#225568 - $15.00 USD Received 24 Oct 2014; revised 2 Dec 2014; accepted 5 Dec 2014; published 28 Jan 2015
© 2015 OSA

Since the Ito integrals have zero mean, the average is the same as in the case of fixed gain. To calculate the fluctuations of ℓ we use Eq. (29) with $f(z') = L - \frac{L}{\alpha_0(L-z')}$, and obtain

$$\sigma_2^2 = \frac{22\sigma_\alpha^4 L^2}{\ln^2(2)180\,(4N^2-1)} - \frac{5\alpha_0 L - 6}{\ln^2(2)12\,(4N^2-1)}\frac{\sigma_\alpha^4}{\alpha_0^2} \tag{35}$$

MDL-free reference system operating at $S'_{\rm ref}$

In this case, the capacity of the MDL-free reference system for large SNR values is

$$C'_{\rm ref} = 2N\log_2\left(S_0\frac{\gamma_0}{\gamma'_0}\right) \tag{36}$$

and, as shown in [5], the capacity loss per mode reduces to the simple expression

$$\ell = \frac{\Gamma^2 - \Gamma'^2}{2\ln(2)} \simeq \frac{1}{2\ln(2)}\left(\gamma^2 - \gamma'^2\right). \tag{37}$$

where the second equality follows from the two equalities $\gamma^2 = \gamma_0^2\Gamma^2$ and $\gamma'^2 = \gamma_0'^2\Gamma'^2$ which, to first order in σ_α^2, simplify to $\gamma^2 \simeq \Gamma^2$ and $\gamma'^2 \simeq \Gamma'^2$. Using the firsts of Eqs. (23) and (25), the above can be expressed as

$$\ell = \frac{1}{2\ln(2)}\left(\int_0^L\int_0^L \mathrm{d}\vec{W}_{z'}\cdot\mathrm{d}\vec{W}_{z''} - \frac{1}{L^2}\int_0^L\int_0^L z'z''\mathrm{d}\vec{W}_{z'}\cdot\mathrm{d}\vec{W}_{z''}\right), \tag{38}$$

which, due to the absence of I and g, shows that the capacity loss is in this case independent of the amplification scheme that is assumed. Using the relation $\langle \mathrm{d}\vec{W}_{z'}\cdot\mathrm{d}\vec{W}_{z''}\rangle = \sigma_\alpha^2\delta(z'-z'')\mathrm{d}z'\mathrm{d}z''$, one can see that the average of the first integral is $\sigma_\alpha^2 L$, while that of the second integral is $\sigma_\alpha^2 L^3/3$, which confirms that the average capacity loss is also in this case $\langle\ell\rangle = \sigma_\alpha^2 L/3\ln(2)$, as already found in [5]. The evaluation of the mean square value of ℓ involves solving the following averages,

$$\begin{aligned}&\left\langle\left[\int_0^L\int_0^L \mathrm{d}\vec{W}_{z'}\cdot\mathrm{d}\vec{W}_{z''}\right]\left[\int_0^L\int_0^L z'z''\mathrm{d}\vec{W}_{z'}\cdot\mathrm{d}\vec{W}_{z''}\right]\right\rangle,\\ &\left\langle\left[\int_0^L\int_0^L \mathrm{d}\vec{W}_{z'}\cdot\mathrm{d}\vec{W}_{z''}\right]^2\right\rangle,\quad \left\langle\left[\int_0^L\int_0^L z'z''\mathrm{d}\vec{W}_{z'}\cdot\mathrm{d}\vec{W}_{z''}\right]^2\right\rangle\end{aligned} \tag{39}$$

which can be done by going through some cumbersome yet conceptually straightforward algebraic procedure which requires using Eqs. (31) and (32). As a result, the variance of ℓ, which in this case we denote by $\sigma_1'^2$, is found to be

$$\sigma_1'^2 = \frac{55\sigma_\alpha^4 L^2}{180\ln^2(2)\,(4N^2-1)} = 55\sigma_1^2. \tag{40}$$

Noise at the receiver

Under the assumption of isotropic noise loading at the receiver the noise coherency matrix reduces to the identity, $\mathbf{Q} = \mathbf{I}$, with the result that $\gamma'_0 = 1$ and $\vec{\gamma}' = 0$. The expression for the capacity loss per mode reduces in this case to

$$\ell_{\rm RX} = \log_2\left(\frac{1}{\langle\gamma_0\rangle}\right) + \frac{1}{2\ln(2)}\left(\frac{1}{\gamma_0^2 - \gamma^2} - 1\right) \simeq \frac{1}{2\ln(2)}\left[2I(0,L) + \sigma_\alpha^2 L\right], \tag{41}$$

#225568 - $15.00 USD Received 24 Oct 2014; revised 2 Dec 2014; accepted 5 Dec 2014; published 28 Jan 2015
© 2015 OSA

where the second equality is obtained by expanding Eq. (17), and where we used the result $\langle \gamma_0 \rangle = 1$, which holds for both amplification schemes 1 and 2. Equation (41) shows that for amplification schemes 1 and 2, owing to the relation $\langle I(0,L) \rangle = 0$, the average capacity loss per mode is $\langle \ell_{\mathrm{RX}} \rangle = \frac{\sigma_\alpha^2 L}{2\ln(2)} = \frac{3}{2}\langle \ell \rangle$. Moreover, for Scheme 1 $I(0,L) = 0$, with the result that $\ell_{\mathrm{RX}} = \frac{1}{2\ln(2)}\sigma_\alpha^2 L$, which shows that to first order in σ_α^2 the capacity loss per is deterministic, consistent with the delta-like PDF in plotted in Fig. 7.

Acknowledgments

C. Antonelli and A. Mecozzi acknowledge financial support from the Italian Ministry of University and Research through ROAD-NGN project (PRIN2010-2011). M. Shtaif acknowledges financial support from Israel Science Foundation (grant 737/12) and the Terasanta consortium.

#225568 - $15.00 USD Received 24 Oct 2014; revised 2 Dec 2014; accepted 5 Dec 2014; published 28 Jan 2015
© 2015 OSA